Title
Quantification of myocardial blood flow using non–ECG-triggered MR imaging

Journal
Magnetic Resonance in Medicine, 74(3)

ISSN
0740-3194

Authors
Chen, David
Sharif, Behzad
Dharmakumar, Rohan
et al.

Publication Date
2015-09-01

DOI
10.1002/mrm.25451

Peer reviewed

HHS Public Access

Author manuscript

Magn Reson Med. Author manuscript; available in PMC 2016 September 01.

Published in final edited form as:

Magn Reson Med. 2015 September ; 74(3): 765–771. doi:10.1002/mrm.25451.

Quantification of Myocardial Blood Flow using Non-ECG-Triggered MR Imaging

David Chen[1,2], **Behzad Sharif**[2], **Rohan Dharmakumar**[2,5], **Louise E.J. Thomson**[3,4], **C. Noel Bairey Merz**[4], **Daniel S. Berman**[2,3], and **Debiao Li**[2,5]

[1]Department of Biomedical Engineering, Northwestern University, Chicago, IL, USA

[2]Biomedical Imaging Research Institute, Department of Biomedical Sciences, Cedars-Sinai Medical Center, Los Angeles, CA, USA

[3]S. Mark Taper Foundation Imaging Center, Department of Imaging, Cedars-Sinai Medical Center, Los Angeles, CA, USA

[4]Barbara Streisand Women's Heart Center, Cedars-Sinai Heart Institute, Los Angeles, CA, USA

[5]David Geffen School of Medicine, University of California, Los Angeles, CA, USA

Abstract

Purpose—MR myocardial perfusion imaging is dependent on reliable electrocardiogram (ECG) triggering for accurate measurement of myocardial blood flow (MBF). A non-ECG-triggered method for quantitative first-pass imaging may improve clinical feasibility in patients with poor ECG signal. The purpose of this study is to evaluate the feasibility of a non-ECG-triggered method for myocardial perfusion imaging in a single slice.

Methods—The proposed non-ECG-triggered technique utilizes a saturation-recovery magnetization preparation and golden-angle radial acquisition for integrated arterial input function (AIF) measurement. Image based self-gating with a temporal resolution of 42.6 ms is used to generate a first-pass image series with consistent cardiac phase. The AIF is measured using beat-by-beat T1 estimation of the ventricular blood pool. The proposed technique was performed on 14 healthy volunteers and compared against a conventional ECG-triggered dual-bolus acquisition.

Results—The proposed method produced MBF with no significant difference compared to ECG-triggered technique (mean of 0.63 ± 0.22 ml/min/g to 0.73 ± 0.21 ml/min/g).

Conclusion—We have developed a non-ECG-triggered perfusion imaging method with T1 based measurement of the AIF in a single slice. In this preliminary study, our results demonstrate that MBF measured using the proposed method is comparable to the conventional ECG-triggered method.

Keywords

myocardial perfusion; flow quantification; ungated acquisition; saturation correction; arterial input function

Correspondence to: Debiao Li, Ph.D., Biomedical imaging Research Institute, Cedars-Sinai Medical Center, 8700 Beverly Blvd, PACT Suite 800W, Los Angeles, CA, USA 90048, Phone: 3104237743, debiao.li@cshs.org.

Introduction

Myocardial perfusion imaging using MR is an important tool for the diagnosis of coronary artery disease (CAD) (1–3). However, despite higher achievable resolution and the lack of ionizing radiation, MR has yet to achieve widespread and routine use for the diagnosis of CAD. One limitation for MR imaging is an accurate and reliable electrocardiogram (ECG) triggering is required to acquire data in the same cardiac phase during every cardiac cycle. Patient physical characteristics (barrel chest) and magnetohydrodynamic effects (particularly at high field such as 3T) can degrade the ECG signal quality, resulting in incorrect or missed triggering. This strict requirement is exacerbated for perfusion imaging, where stress imaging may worsen heart rate variability and arrhythmias, leading to skipped cardiac cycles and potentially losing diagnostically critical information.

Beyond qualitative imaging, skipped cardiac cycles can result in errors in myocardial blood flow (MBF) quantification. Quantification of MBF has the potential to give unique information towards the diagnosis of triple-vessel disease and microvascular disease in comparison to simple qualitative evaluation (4–6). However, accurate measure of MBF requires single cardiac cycle temporal resolution (7). Furthermore, triggering in a consistent cardiac phase is important to maintain simple segmentation. Excessive cardiac motion due to mistriggering requires manual manipulation of myocardial contours. Sensitivity to motion can increase workflow complexity; greatly hindering the clinical utility of quantitative MR perfusion imaging.

One recent advance aimed at addressing this issue is the development of non-ECG triggered imaging (8,9). Instead of relying on the ECG or other physiological signals, the triggering signal is derived directly from the acquired data. Non-ECG-triggered cardiac MR imaging has been shown to produce diagnostically useful images in patients with severe arrhythmias who normally would have been excluded from a CMR study (10–14). With respect to myocardial perfusion imaging, non-triggered imaging has been shown to be robust to various arrhythmias which may yield non-diagnostic images with a conventional gated approach (9).

To address the sensitivity of MR imaging to ECG mistriggering, we propose a non-ECG-triggered sequence with integrated T1 AIF measurement for quantitative myocardial perfusion measurement using a single bolus. Integrated AIF measurement using single-cardiac-cycle fast T1 mapping is used to correct for the nonlinear relationship between blood signal intensity and Gadolinium concentration in the arterial input function (AIF) (15–17). Unlike the two more prominent methods in measuring the AIF (the “dual-bolus” (18,19) and the “dual sequence” (20,21) methods), the integrated T1 AIF measurement acquires the true AIF without the need to acquire a separate scan or increase the acquisition window. The aim of this study was to evaluate the feasibility of this method in a healthy volunteer population.

Methods

Acquisition and Reconstruction

Conventional ECG-triggered first pass pulse sequences typically use a saturation recovery magnetization preparation (SR-preparation) followed by either a Cartesian gradient recalled echo (GRE) or balanced steady-state free precession readout at a predetermined TI time for each slice (as shown in Figure 1a). Due to the dependence on ECG-triggering to maintain a consistent cardiac phase, poor ECG signal or highly variable heart rates result in skipped beats or inconsistent cardiac phase between cardiac cycles. In a non-triggered acquisition scheme (Figure 1b), data is continuously acquired without pause or need for an ECG signal. Following reconstruction, a perfusion image series is then generated by binning into different cardiac phases.

Previously published non-ECG-triggered perfusion imaging methods include steady-state acquisition approaches (8,14,22). Steady-state imaging has been shown to exacerbate the nonlinearity between contrast agent concentration and signal intensity compared to SR-prepared, GRE acquisitions; further reducing the accuracy of MBF measurements (22). The focus of this work is to develop a method for accurate measurement of MBF using a non-ECG-triggered acquisition. The proposed 2D sequence (as depicted in figure 1b) uses SR-preparation in conjunction with radial golden angle GRE acquisition to enable fast T1 mapping for integrated AIF measurement.

One advantage of using golden angle trajectory is the ability to retrospectively determine the reconstruction window. In the proposed method, a sliding window length of 64 projections (acquisition window of 140 ms) was shifted by 21 projections resulting in a temporal resolution of 40 ms (~25 frames per second). The images were reconstructed using non-Cartesian SENSE (as shown in Figure 2a) (23). In lieu of the ECG, the ventricular blood pool size was used to identify the proper cardiac phase. The gating signal was generated from the average signal in a region of interest (ROI) drawn over the heart (9). The average signal in this ROI corresponds to the size of the blood pool: higher signal correlates to the larger blood pool during end-diastole while lower signal correlates with the small blood pool during end-systole (as shown in Figure 2b). Peak detection is used to identify the peaks and valleys in the signal.

Integrated, single-bolus AIF measurement was accomplished through direct measurement of contrast agent concentration during each cardiac cycle using beat-by-beat T1 estimation. Single cardiac cycle T1 estimation is accomplished by measuring the longitudinal relaxation following a typical SR magnetization preparation during first-pass perfusion exam. Tissue parameters such as T1 and proton density can be solved for using the known acquisition parameters and relaxation model derived from the Bloch equation (17,24):

$$s=\rho[(1-e^{-T1/T1})(E\cos(\alpha))^{n-1}+(1-E)\frac{1-(E\cos(\alpha))^{n-1}}{1-E\cos(\alpha)} \quad \text{(Eq. 1)}$$

Where ρ includes contribution from proton density, T2* relaxation and coil sensitivity variations; $E = e^{-TR/T1}$, α = flip angle, n = number of imaging RF pulses applied before

acquiring the center line of k-space; and TI = delay time. Although radial imaging does not have a well-defined TI because the k-space center is traversed during every projection, the TI can be well approximated if the reconstruction window includes a limited number of projections (17). T1, ρ, and α were solved for using a nonlinear least squares solver in MATLAB (Mathworks, Natick, MA). The α was included in the fitting procedure as B1 inhomogeneities likely causes the actual experienced by the imaged tissue to be significantly different α as the specified in the protocol. The T1 values were then be converted to contrast agent concentration using the known relaxivity of gadolinium-based contrast agent ($\gamma = 3.9$ $mM^{-1}s^{-1}$):

$$\frac{1}{T_1} = \frac{1}{T_{1baseline}} + \gamma[Gd] \quad \text{(Eq. 2)}$$

Acquisition was started immediately following the SR-preparation to capture the fast relaxation of blood during peak contrast during first-pass studies. To sample the longitudinal relaxation with enough temporal resolution to capture longitudinal relaxation dynamics, a short reconstruction window is needed. Images were reconstructed using 21 projections with non-Cartesian SENSE for T1 measurement images. Resolution requirements are significantly relaxed for the images used to measure T1 because the AIF is found using a large ROI drawn in the left ventricular blood pool. As such, the data was apodized using a Gaussian filter to minimize streaking, resulting in an effective resolution of 5.1×5.1 mm^2. An end diastolic phase was retrospectively selected to further minimize resolution requirements by maximizing the size of the ventricular blood pool. Although a series of T1 measurement images can overlap a SR-preparation (as with the high resolution image shown in Figure 1), individual images do not overlap the preparation pulse. As such, each T1 mapping image retains a defined contrast sampling along the longitudinal relaxation curve. Unlike previous work (15–17), a sliding window of 10 projections was used to increase the effective temporal resolution; thereby increasing the number of samples (5 T1 estimation images with a temporal resolution of 24.2 ms) and improve the conditioning of the fit.

Imaging protocols

Fourteen healthy volunteers (4 males, 10 females) with an average age of 31.1±10.7 years old underwent perfusion MRI studies on a Siemens 3T Verio (Siemens Medical Solutions, Erlangen, Germany) system with IRB approval and written informed consent. Studies employed a 12-channel spine and body phased-array coil. Two first-pass perfusion scans were performed at rest. The first scan was performed using a conventional ECG-triggered SR-prepared Cartesian sequence with a GRE readout. The second scan was performed using the proposed non-ECG-triggered SR-prepared GRE pulse sequence with golden angle radial acquisition for T1 mapping. The scans used a commercially available composite pulse train SR preparation as described previously (25). A single midventricular slice was acquired. Subjects were given a bolus of 0.05 mmol/kg Optimark (gadoverstamide injection, Mallinckrodt Inc, Montana, USA) followed by a 20 ml saline flush at a rate of 4 ml/s. To minimize respiratory motion, both full bolus scans were performed during breath-hold.

The dual-bolus method was performed first to minimize the impact of residual contrast agent on the dilute bolus. A three-way valve was placed on saline side of the power injector. The line was flushed with saline. A 1/10 dilute bolus (0.005 mmol/kg) was then injected into the line through the 3-way valve. Prior to the first scan, a dilute bolus was first injected using a 20 ml saline flush. A 25 frame (total scan time ~22s) free-breathing ECG-triggered Cartesian scan was run while the volunteer was asked to breathe shallowly. Immediately following the end of dilute scan, the subject was immediately hyperventilated and asked to perform a breath-hold for a typical first-pass study with a 40 frame (total scan time ~36s) ECG-triggered Cartesian scan. Following a 10 minute period for residual contrast to wash out, a second rest perfusion scan was run using the proposed non-ECG-triggered radial method with a breath-hold.

Imaging parameters for the ECG-triggered scan are as follows: Cartesian trajectory, FOV = 300 mm^2; bandwidth = 697 Hz/pixel; flip angle = 12°; TR/TE = 2.5/1.1 ms; spatial resolution = 2.0×3.0×8mm^3; 160 readout by 40 phase encodes; TGRAPPA Rate = 2. Imaging parameters for the non-ECG-triggered scan are as follows: FOV = 270 mm^2; bandwidth = 911 Hz/pixel; flip angle = 12°; TR/TE = 2.2/1.2 ms; spatial resolution = 1.7×1.7×8 mm^3, 160 readout points by 64 projections collected with a golden angle trajectory were acquired immediately following the SR preparation. 210 repetitions were collected over 34 seconds.

Analysis

Segmentation was conducted using custom code written in MATLAB. The ROI in the ventricular blood pool was drawn to avoid papillary muscle. Online image registration was employed for the triggered scans to minimize the effects of respiratory motion (26). The ROI in the myocardium was divided into AHA recommended segments (27). Image signal intensity over time curves of the LV cavity and the myocardial sectors were generated for the dilute bolus and normal concentration triggered datasets and each TI of the non-ECG-triggered radial datasets. Average MBF was measured in each segment.

Estimates of MBFs were found for both the dual-bolus ECG-triggered and single-bolus non-ECG-triggered acquisitions. The MBF of the ECG-triggered image series was found using the AIF measured from the dilute bolus scan. The “dilute” AIF was scaled by the dilution factor 10-fold) to match the signal intensity of the full bolus myocardial time curves. In lieu of a separate, dilute bolus scan, the true AIF for the non-ECG-triggered acquisition was found using an integrated T1 estimation method, as previously described. Due to the difference in units between this single-bolus “T1-derived” AIF and the myocardial tissue function (contrast agent concentration compared to signal intensity), the “T1-derived” AIF has to be converted back to the original units of signal intensity. The scaling was found by taking the average of the last 4 points of the “T1-derived” AIF and normalized to the average of the last 4 points of the signal intensity AIF (15,16). The scaled “T1-derived” AIF was then used to find the MBF for the single bolus non-ECG-triggered acquisition.

MBFs were found using a linear time invariant model with a model independent deconvolution (28). All signal curves were truncated to include only first-pass to minimize effects of incomplete breath-hold. Paired Student’s t-test was performed comparing

estimated MBF of the whole myocardium derived from image signal intensities and the proposed T1 estimation method. The statistical significance was set at $p = 0.05$. The similarity in measured MBF values (proposed non-ECG-triggered integrated T1-derived AIF vs ECG-triggered dual-bolus) was analyzed using Bland-Altman plots.

Results

Figure 2a shows representative first-pass perfusion images. Images from multiple cardiac phases are shown for different phases of contrast passage. Figure 2b shows the gating signal produced from image signal intensities. End systolic and end systolic cardiac phases are identified using peak detection, with additional cardiac phases binned. Non-ECG-triggered radially acquired images have higher in-plane resolution compared to the ECG-triggered Cartesian imaging (1.7×1.7 mm^2 to 2.9×1.9 mm^2). The corresponding movies of the first-pass series is provided in Supplemental Material available in the online version of this article. Figure 3a shows the images of different “times to the center projection” used for T1 mapping for the integrated AIF measurement during different phases of contrast passage. The windowing is kept at the same level for each image. Effective resolution of these images is 5.1×5.1 mm^2. The mean image signal intensity measured in an ROI drawn in the ventricular blood pool is shown. The fitted relaxation curve is also shown for different phases of contrast passage (Figure 3b and 3c).

Figure 4 shows a comparison of AIFs (4a) and myocardial tissue (4b) curves between the ECG-triggered, dual-bolus and non-ECG-triggered, T1 derived integrated acquisitions. The derived curves have been rescaled to fit on the same y-axis to show the similarity between the two methods. The AIFs show a significant increase 60 ± 15% when compared to AIFs measured directly from the raw signal intensities. The mean peak T1 found across all scans is 56 ± 12 ms. The mean MBF across 14 subjects found using the gold standard dual-bolus protocol and the proposed non-ECG-triggered protocol were 0.73 ± 0.21 ml/min/g and 0.63 ± 0.22 ml/min/g respectively. There was no significant difference between the two methods ($p=0.21$). Figure 5a shows the correlation between the MBF in AHA segments found using the conventional dual-bolus and proposed integrated T1 mapping. The correlation coefficient was found to be 0.964 with a linear correlation of $MBF_{integrated} = 0.940\ MBF_{dual\text{-}bolus} - 0.143$. Figure 5b shows Bland-Altman plot. There is a slight, but statistically significant underestimation (0.10 ± 0.06 ml/min/g) of MBF using the proposed method compared to the dual-bolus method.

Discussion

The need for accurate and reliable ECG gating for quantitative myocardial perfusion imaging can impact the accuracy of MBF estimates. Mistriggering due to a poor ECG signal can cause inconsistent segmentation and/or loss of temporal resolution, resulting in poor MBF estimates (7). This is especially of a concern in a patient population which suffers from inconsistent sinus rhythm. As shown previously, non-ECG-triggered imaging increases the robustness of perfusion MR to arrhythmias (9). In this work, a method for non-ECG-triggered quantification of MBF with integrated AIF measurement using beat-by-beat T1 estimation of the AIF for a single slice was developed. The results show feasibility of using

a non-ECG-triggered sequence to measure MBF without the need for an additional dilute bolus.

The image based gating method used in this study was successfully implemented. A consistent end-systolic and mid-diastolic cardiac phase was identified for all volunteers during first-pass of the contrast agent. Furthermore, anecdotal evidence suggests that identifying a consistent systolic and diastolic phase was possible even during shallow breathing. The gating signal is not dependent on the absolute magnitude (size of the ventricles) but rather the change in magnitude within a single cardiac cycle. This combined with the slow rate of respiratory motion in comparison with cardiac motion results in a gating signal that is robust to respiratory motion. The results are in concordance with the study done by Harrison and Dibella which employed a similar self-gating method with a free-breathing protocol (9).

MBF found using the proposed method slightly underestimates MBF compared to the reference dual-bolus technique (as shown in figure 5b). This underestimation is likely due to the dual-bolus scan being acquired first in each study. Though residual contrast agent in the blood is significantly lower compared to during peak contrast, and the baseline amount is subtracted out before being deconvolved with the AIF, it is possible that the residual contrast agent contributes to saturation of the signal intensity in the myocardium during the second injection. This would lead to a lower than expected MBF measurement. Another potential cause for discrepancy of these two methods is the changing hemodynamic conditions between the dilute and normal bolus of the reference dual-bolus method. The dilute bolus was scanned while the volunteers were instructed to undergo shallow breathing. As a result, average heart rates during the dilute bolus were 5–10% slower than during the breath-hold full concentration bolus. The slower heart rate could have caused a lower than expected peak signal intensity, resulting in a slight overestimation of MBF.

Integrated AIF measurement was used because it has a clear workflow advantage over a typical dual-bolus technique for AIF measurement. An additional 6.9 ± 1.5 min in setup time was required to setup a commercially available power injector to run the dual-bolus method at a highly experienced site (King’s College London) (29). This is in concordance with our own experiences with the dual-bolus method. Increasing scan time and setup complexity is highly undesirable due to the already lengthy and complex cardiac examination. Combined with further developments in non-ECG-triggered acquisition for other sequences (14) (30), an additional 3–4 min may be saved by removing the need to setup an ECG.

In addition, with regard to the accuracy of the dual-bolus method, changes to cardiac output or heart rate between the dilute bolus and the full bolus can affect measured MBF. A low ejection fraction may also be a contraindication to this method as the dilute bolus may overlap with the full bolus due to slow passage of the contrast agent (29). Though increasing the pause between the injection of the dilute and full bolus can resolve the two curves, this requires the technologist to be aware of the low ejection fraction prior to the scan.

Compared to the dual sequence method, the proposed method is not sensitive to T2* effects. T2* can cause as much as 20% reduction in peak AIF magnitude perpetuating into similar

magnitude error in the MBF measurement (31). Furthermore, the dual sequence method requires an additional scan of ~50 ms (30% increase in acquisition window). The increase in acquisition window compromises the temporal resolution of the gating signal, potentially sacrificing the ability to resolve each cardiac phase during every cardiac cycle.

Direct measurement of contrast agent concentration of the AIF was accomplished by beat-by-beat estimation of T1. Single cardiac cycle estimation of T1 is achievable due to the short T1 times seen during first pass (50–400ms) (17). The longitudinal relaxation curve can be sufficiently sampled to perform an accurate fit for T1 values in the span of the acquisition time. As with any nonlinear fitting, the condition of this fit (and thus the accuracy of the estimated T1 values) is largely dependent on the number of samples. Compared to previously published T1-derived AIF measurement methods, the proposed method samples the longitudinal magnetization relaxation curve more densely (temporal resolution of 24.2 ms vs 64 ms). This is attributed to using a golden-angle trajectory which allows for arbitrary definition of the reconstruction window and sliding window type reconstruction. As it is shown in Figure 3, though data is shared, the resulting data still conforms well to the theoretical GRE recovery model. It has also been shown in simulations that increased temporal resolution results in better conditioning of the fit and increased robustness to noise (17).

Also included in the nonlinear fit is the flip angle. B1 inhomogeneity causes the true flip angle to be slightly different from the prescribed angle, changing the longitudinal relaxation profile. In this work, the nonlinear fit is overdetermined with 5 high SNR samples of the longitudinal relaxation, which was used to fit for 3 unknowns (T1, proton density, and flip angle). A separate B1 measurement scan can be used to reduce the number of unknowns in the fit, improving the condition and confidence in the fit. However, adding a B1 measurement would increase exam time, workflow complexity, and adds to patient discomfort.

In this work, T1 estimation images acquired during end-diastole were selected for AIF measurement. This was done to minimize the required spatial resolution needed to reconstruct the ventricular blood pool without significant undersampling artifact. It is also possible to measure the AIF during end-systole. The resolution requirements for end-systole are not significantly more stringent compared to end-diastole. Motion is not a major concern due to the short reconstruction window (46.2 ms) of each T1 estimation image and the robustness of radial trajectory to motion. The ability to acquire an AIF during different cardiac phases is important because the AIF may be different depending on which cardiac phase it was acquired from (32). Another concern for T1 estimation is through-plane blood flow which may disrupt the longitudinal relaxation. This is minimized by selecting end-diastole (as was done in this work) or end-systole.

To enable integrated T1 estimation, a SR-preparation is used. One consequence of this is that compared to steady-state imaging, the reconstruction window may cross a SR-preparation, resulting in large variation in image energy for sequential projections. If the projections were incremented linearly (i.e. 0°, 3°, 6°, etc.), the image would have been essentially filtered due to the modulation in k-space caused by the longitudinal recovery.

However, because projections are incremented by 111.25°, projections of low energy are approximately evenly spaced throughout k-space, reducing streaking artifacts. Another result of using the SR-preparation is that, the length of the reconstruction window is pre-determined by the number of projections taken after each SR preparation. This is to ensure each that image has consistent T1 weighting because not every projection has equal T1 weighting.

One possible disadvantage of the unequal T1 weighting of each projection is that the images may be inappropriate for use for cine imaging. Although the reported temporal resolution of the gating signal is comparable to cine imaging at 40 ms (25 frames per second), the image series during a single cardiac cycle may not capture true cardiac motion. The projections immediately following the SR-preparation contain very little energy, and thus contribute very little to the reconstruction of the image. Though this sequence may not be appropriate for diagnostic cine imaging, it is adequate for the purpose of triggering. Within a cardiac cycle, only a relative measure of motion is needed to find end-systolic or end-diastolic phase.

Study limitations

The results presented in this proof-of-concept work were limited to single-slice imaging at rest. Conventional myocardial perfusion imaging typically requires 3–4 short axis slices during stress. Extension of the technique to multi-slice imaging for clinical application may be possible with further accelerated acquisition, as only parallel imaging is used in this work. We have recently demonstrated the feasibility of using an integrated AIF measurement for quantifying myocardial perfusion with 8-fold temporal acceleration (17). This method is also needs to be validated for stress imaging. However, similar methods have been shown to be applicable to stress imaging and at high heart-rates (14,22,33).

Conclusions

In this preliminary study, we developed and evaluated a non-ECG-triggered method for myocardial perfusion quantification. The results in healthy volunteers demonstrate that the proposed method is capable of producing myocardial blood flow measurements with no significant differences compared to ECG triggered dual-bolus technique. The proposed non-ECG triggered method requires only a single injection of contrast agent which simplifies the workflow for quantitative myocardial perfusion studies.

Supplementary Material

Refer to Web version on PubMed Central for supplementary material.

Acknowledgements

This projected was supported in part by NIH grant numbers T32 EB51705 and RO1 EB002623, NIBIB grant number EB002623, AHA Scientist Development Grant 14SDG20480123, GCRC grant MO1-RR00425, and Edythe L. Broad Women’s Heart Research Fellowship UN55ES6580F.

References

1. Greenwood JP, Maredia N, Younger JF, Brown JM, Nixon J, Everett CC, Bijsterveld P, Ridgway JP, Radjenovic A, Dickinson CJ, Ball SG, Plein S. Cardiovascular magnetic resonance and single-photon emission computed tomography for diagnosis of coronary heart disease (CE-MARC): a prospective trial. Lancet. 2012; 379(9814):453–460. [PubMed: 22196944]
2. Schwitter J, Wacker CM, Wilke N, Al-Saadi N, Sauer E, Huettle K, Schonberg SO, Luchner A, Strohm O, Ahlstrom H, Dill T, Hoebel N, Simor T. Investigators M-I. MR-IMPACT II: Magnetic Resonance Imaging for Myocardial Perfusion Assessment in Coronary artery disease Trial: perfusion-cardiac magnetic resonance vs. single-photon emission computed tomography for the detection of coronary artery disease: a comparative multicentre, multivendor trial. Eur Heart J. 2013; 34(10):775–781. [PubMed: 22390914]
3. Schwitter J, Wacker CM, van Rossum AC, Lombardi M, Al-Saadi N, Ahlstrom H, Dill T, Larsson HB, Flamm SD, Marquardt M, Johansson L. MR-IMPACT: comparison of perfusion-cardiac magnetic resonance with single-photon emission computed tomography for the detection of coronary artery disease in a multicentre, multivendor, randomized trial. Eur Heart J. 2008; 29(4): 480–489. [PubMed: 18208849]
4. Camici PG, Rimoldi OE. The Clinical Value of Myocardial Blood Flow Measurement. J Nucl Med. 2009; 50(7):1076–1087. [PubMed: 19525470]
5. Lee DC, Johnson NP. Quantification of absolute myocardial blood flow by magnetic resonance perfusion imaging. J Am Coll Cardiol. 2009; 2(6):761–770.
6. Wang L, Jerosch-Herold M, Jacobs DR Jr, Shahar E, Detrano R, Folsom AR. Coronary artery calcification and myocardial perfusion in asymptomatic adults: the MESA (Multi-Ethnic Study of Atherosclerosis). J Am Coll Cardiol. 2006; 48(5):1018–1026. [PubMed: 16949496]
7. Kroll K, Wilke N, Jerosch-Herold M, Wang Y, Zhang Y, Bache RJ, Bassingthwaighte JB. Modeling regional myocardial flows from residue functions of an intravascular indicator. The American journal of physiology. 1996; 271(4):H1643–H1655. [PubMed: 8897962]
8. DiBella EV, Chen L, Schabel MC, Adluru G, McGann CJ. Myocardial perfusion acquisition without magnetization preparation or gating. Magn Reson Med. 2012; 67(3):609–613. [PubMed: 22190332]
9. Harrison A, Adluru G, Damal K, Shaaban AM, Wilson B, Kim D, McGann C, Marrouche NF, Dibella EV. Rapid ungated myocardial perfusion cardiovascular magnetic resonance: preliminary diagnostic accuracy. J Cardiovasc Magn Reson. 2013; 15(1):26. [PubMed: 23537093]
10. Larson AC, White RD, Laub G, McVeigh ER, Li D, Simonetti OP. Self-gated cardiac cine MRI. Magn Reson Med. 2004; 51(1):93–102. [PubMed: 14705049]
11. Kellman P, Epstein FH, McVeigh ER. Adaptive sensitivity encoding incorporating temporal filtering (TSENSE). Magn Reson Med. 2001; 45(5):846–852. [PubMed: 11323811]
12. Bassett EC, Kholmovski EG, Wilson BD, DiBella EV, Dosdall DJ, Ranjan R, McGann CJ, Kim D. Evaluation of highly accelerated real-time cardiac cine MRI in tachycardia. NMR Biomed. 2014; 27(2):175–182. [PubMed: 24259281]
13. Zhang S, Uecker M, Voit D, Merboldt KD, Frahm J. Real-time cardiovascular magnetic resonance at high temporal resolution: radial FLASH with nonlinear inverse reconstruction. J Cardiovasc Magn Reson. 2010; 12:39. [PubMed: 20615228]
14. Sharif B, Dharmakumar R, Arsanjani R, Thomson LE, Merz N, Berman DS, Li D. Ungated cine first-pass CMR for concurrent imaging of myocardial perfusion defects and wall motion abnormalities. J Cardiov Magn Reson. 2013; 15(Suppl 1):O1.
15. Kholmovski EG, DiBella EV. Perfusion MRI with radial acquisition for arterial input function assessment. Magn Reson Med. 2007; 57(5):821–827. [PubMed: 17457875]
16. Kim TH, Pack NA, Chen L, DiBella EV. Quantification of myocardial perfusion using CMR with a radial data acquisition: comparison with a dual-bolus method. J Cardiovasc Magn Reson. 2010; 12:45. [PubMed: 20653961]
17. Chen D, Sharif B, Dharmakumar R, Thomson LEJ, Bairey Merz CN, Berman DS, Li D. Improved quantification of myocardial blood flow using highly constrained back projection reconstruction. Magnetic Resonance in Medicine. 2013 In Press, 10.1002/mrm.24958.

18. Hsu LY, Rhoads KL, Holly JE, Kellman P, Aletras AH, Arai AE. Quantitative myocardial perfusion analysis with a dual-bolus contrast-enhanced first-pass MRI technique in humans. J Magn Reson Imaging. 2006; 23(3):315–322. [PubMed: 16463299]
19. Christian TF, Aletras AH, Arai AE. Estimation of absolute myocardial blood flow during first-pass MR perfusion imaging using a dual-bolus injection technique: comparison to single-bolus injection method. J Magn Reson Imaging. 2008; 27(6):1271–1277. [PubMed: 18421683]
20. Gatehouse PD, Elkington AG, Ablitt NA, Yang GZ, Pennell DJ, Firmin DN. Accurate assessment of the arterial input function during high-dose myocardial perfusion cardiovascular magnetic resonance. J Magn Reson Imaging. 2004; 20(1):39–45. [PubMed: 15221807]
21. Kim D, Axel L. Multislice, dual-imaging sequence for increasing the dynamic range of the contrast-enhanced blood signal and CNR of myocardial enhancement at 3T. J Magn Reson Imaging. 2006; 23(1):81–86. [PubMed: 16331593]
22. Sharif B, Dharmakumar R, Arsanjani R, Thomson L, Bairey Merz CN, Berman DS, Li D. Non-ECG-gated myocardial perfusion MRI using continuous magnetization-driven radial sampling. Magn Reson Med. 2014 In Press.
23. Pruessmann KP, Weiger M, Bornert P, Boesiger P. Advances in sensitivity encoding with arbitrary k-space trajectories. Magn Reson Med. 2001; 46(4):638–651. [PubMed: 11590639]
24. Cernicanu A, Axel L. Theory-based signal calibration with single-point T1 measurements for first-pass quantitative perfusion MRI studies. Acad Radiol. 2006; 13(6):686–693. [PubMed: 16679270]
25. Kim D, Gonen O, Oesingmann N, Axel L. Comparison of the effectiveness of saturation pulses in the heart at 3T. Magn Reson Med. 2008; 59(1):209–215. [PubMed: 18050347]
26. Chefd'hotel C, Hermosillo G, Faugeras O. Flows of diffeomorphisms for multimodal image registration. IEEE International Symposium on Biomedical Imaging. 2002:753–756.
27. Cerqueira MD, Weissman NJ, Dilsizian V, Jacobs AK, Kaul S, Laskey WK, Pennell DJ, Rumberger JA, Ryan T, Verani MS. Myoca AHAWG. Standardized myocardial segmentation and nomenclature for tomographic imaging of the heart: A statement for healthcare professionals from the Cardiac Imaging Committee of the Council on Clinical Cardiology of the American Heart Association. J Am Soc Echocardiog. 2002; 15(5):463–467.
28. Jerosch-Herold M, Swingen C, Seethamraju RT. Myocardial blood flow quantification with MRI by model-independent deconvolution. Med Phys. 2002; 29(5):886–897. [PubMed: 12033585]
29. Ishida M, Schuster A, Morton G, Chiribiri A, Hussain S, Paul M, Merkle N, Steen H, Lossnitzer D, Schnackenburg B, Alfakih K, Plein S, Nagel E. Development of a universal dual-bolus injection scheme for the quantitative assessment of myocardial perfusion cardiovascular magnetic resonance. J Cardiovasc Magn Reson. 2011; 13:28. [PubMed: 21609423]
30. Pang J, Li D. Self-gated 4D whole-heart imaging. J Cardiov Magn Reson. 2014; 16(Suppl 1):W24.
31. Kellman P, Aletras AH, Hsu LY, McVeigh ER, Arai AE. T2* measurement during first-pass contrast-enhanced cardiac perfusion imaging. Magn Reson Med. 2006; 56(5):1132–1134. [PubMed: 17029226]
32. Radjenovic A, Biglands JD, Larghat A, Ridgway JP, Ball SG, Greenwood JP, Jerosch-Herold M, Plein S. Estimates of systolic and diastolic myocardial blood flow by dynamic contrast-enhanced MRI. Magn Reson Med. 2010; 64(6):1696–1703. [PubMed: 20928890]
33. Sharif B, Arsanjani R, Shalev A, Dharmakumar R, Bairey Merz C, Berman DS, Li D. Dark-rim-free ungated first-pass perfusion CMR with 3-Slice end-systolic imaging: initial experience. J Cardiovasc Magn Reson. 2014; 16(Suppl 1):P177.

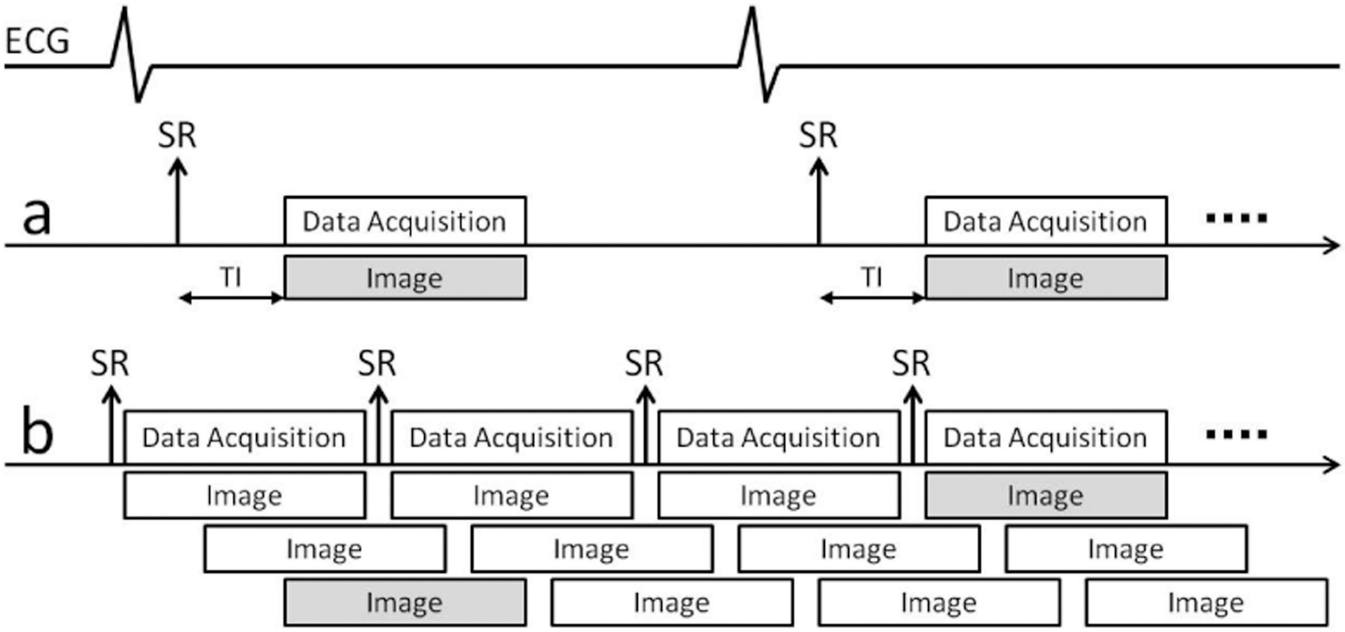

Figure 1.

Schematic of the proposed perfusion imaging method. (**a**) A conventional ECG-triggered perfusion sequence with a predefined trigger time: If the length of the cardiac cycle changes significantly, images may fall outside of the predefined acquisition window. (**b**) Proposed non-ECG-triggered sequence: SR-prepared GRE acquisition is repeated continuously. Each module is 160 ms long, with the acquisition window being 140 ms. A golden angle radial trajectory is used to facilitate a sliding-window reconstruction. To generate the first-pass image series, a consistent cardiac phase is retrospectively identified for each cardiac cycle.

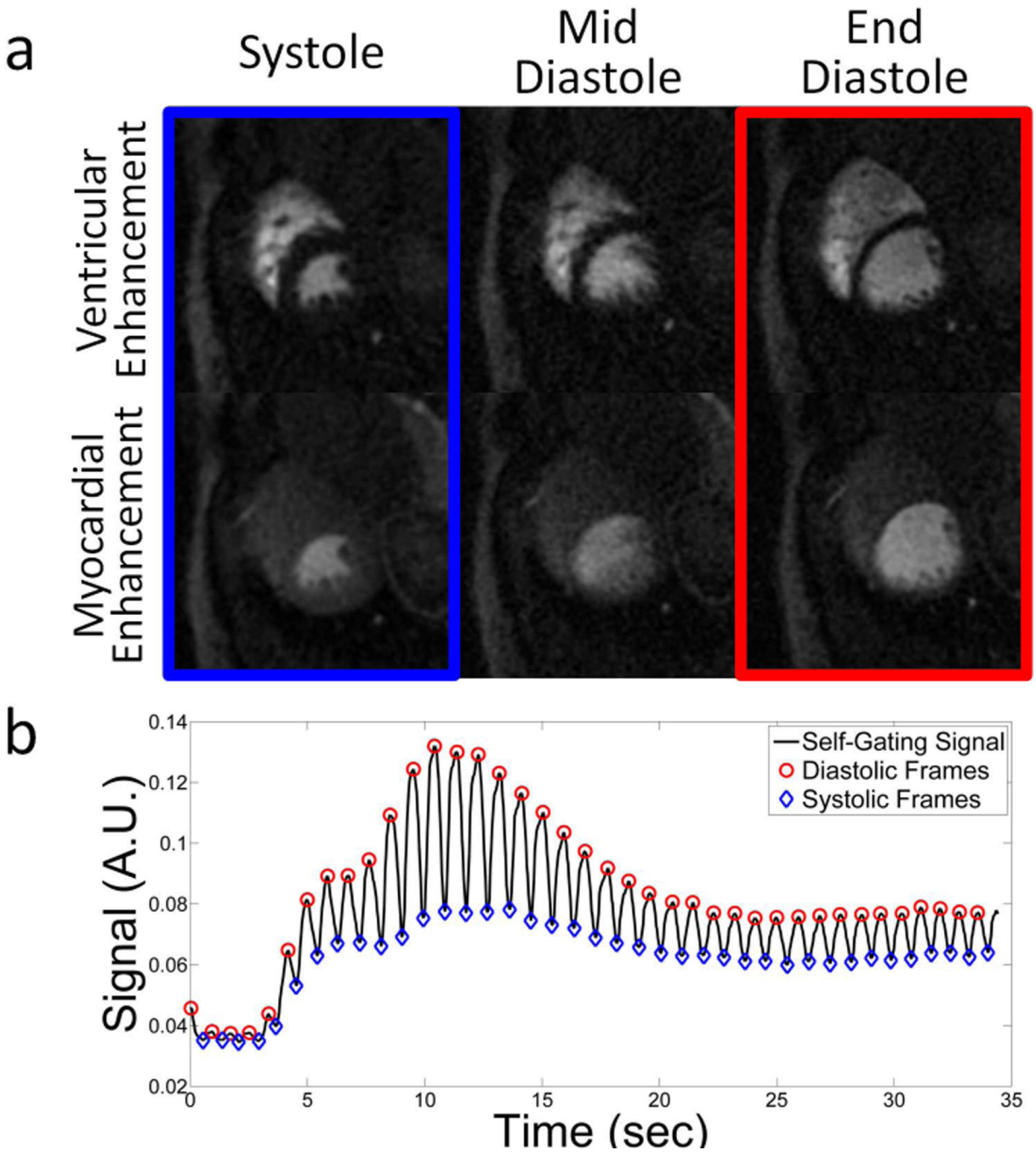

Figure 2.

Representative high resolution images (1.7×1.7 mm^2) and description of the method used to bin image in cardiac phases. (**a**) Images are generated using non-Cartesian SENSE with a sliding window reconstruction. (**b**) The self-gating signal produced from average signal in a ROI surrounding the heart. Peaks correspond to diastole where the large ventricular blood pool produces high signal intensity. Conversely, low signal intensities correspond to the smaller ventricular blood pool during systole. Images are then retrospectively binned into different cardiac phases (shown from ventricular and myocardial enhancement phases).

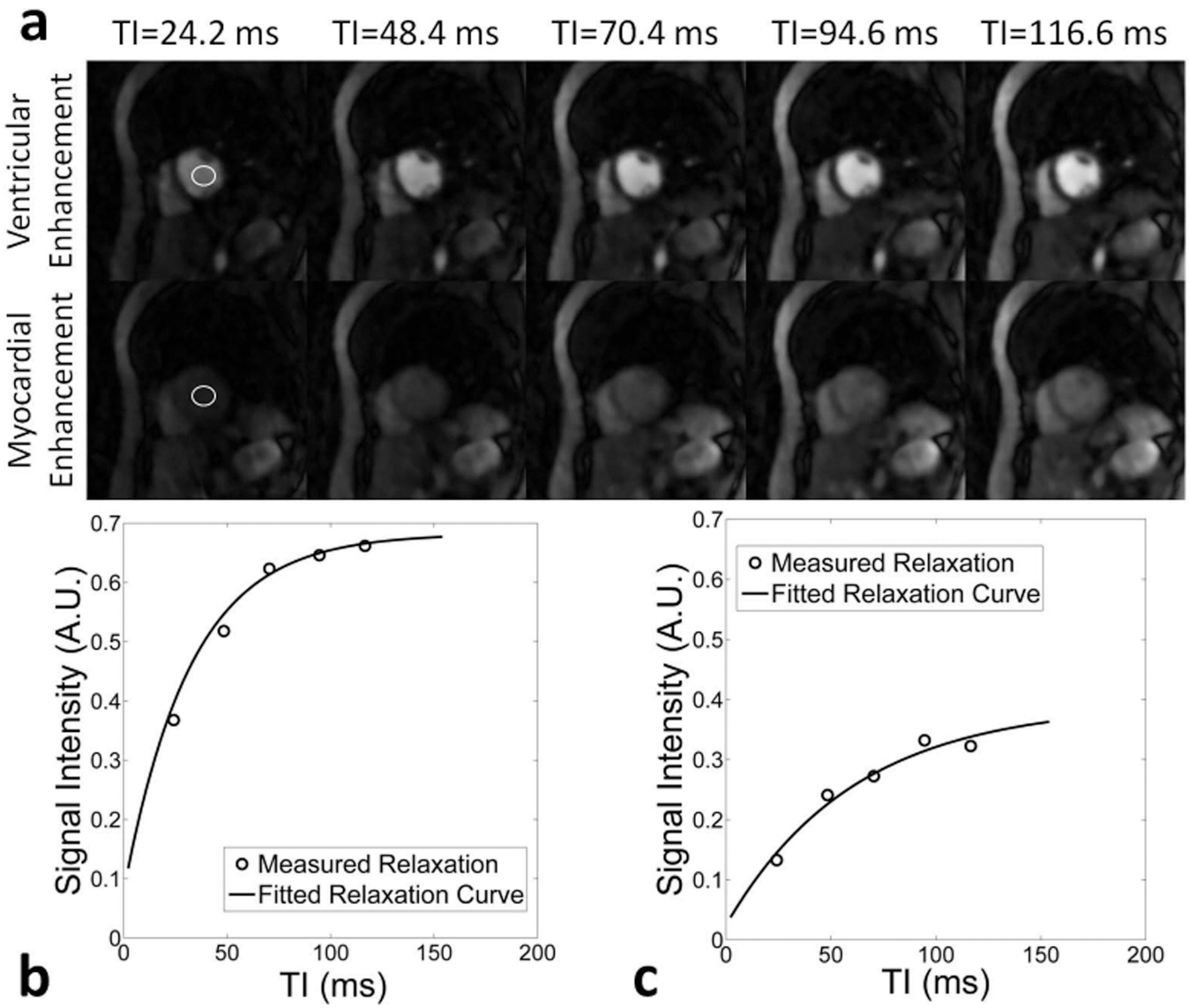

Figure 3.

Description of the T1 estimation method used for accurate measurement of the AIF. Stated times refer to the time from the first projection to the center projection of the image. (**a**) Low resolution images (5.1×5.1 mm^2) used for T1 mapping. Diastolic images are used to reduce the resolution requirements. Images were selected from the peak ventricular enhancement and myocardial enhancement phases. A total of 21 projections are used to produce images from each frame. The nonlinear fit for the T1 recovery curve (Signal intensity of the ventricular blood pool vs TI) in the (**b**) ventricular enhancement phase and (**c**) the myocardial enhancement phase.

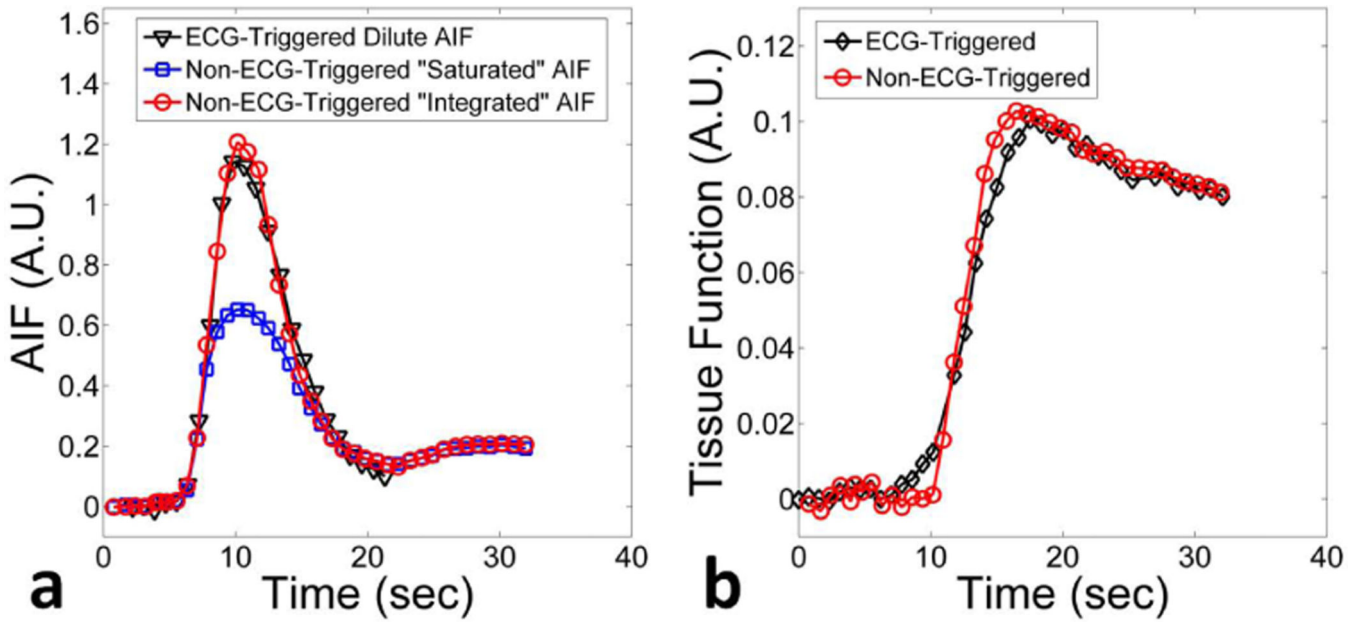

Figure 4.

Example AIF and tissue curves in one subject. All curves have been scaled to fit on the same axis. (**a**) The AIF measured using T1-estimation in the ventricular blood pool (▽) using the proposed non-ECG triggered method, compared with that derived from the dual-bolus (□) method. For comparison, the AIF resulting from raw signal intensity (○) of the non-ECG gated perfusion series is also shown. Due to correction of nonlinearities (saturation effects) of the blood signal, peak of the T1-derived AIF is significantly increased compared to the one corresponding to raw signal intensities. (**b**) Comparison of the myocardial signal curves derived from the non-ECG-triggered and the ECG-triggered images are similar.

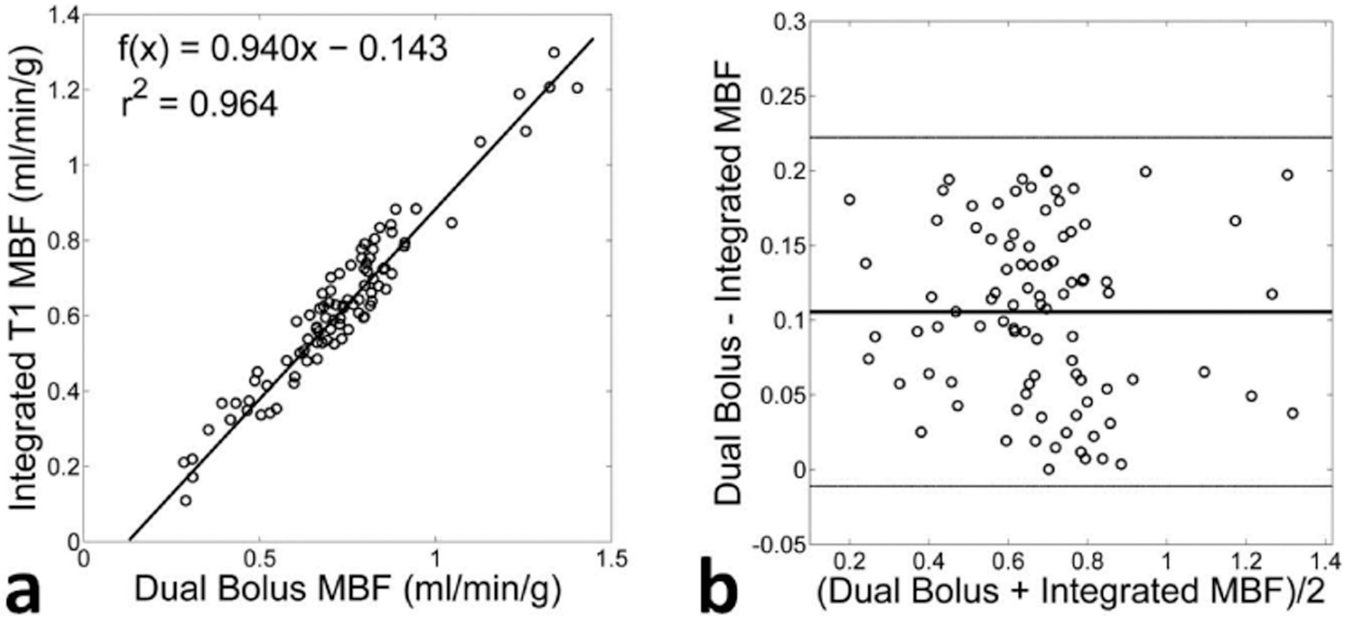

Figure 5.

Comparison of the MBF of the 6 AHA segments found using the proposed non-ECG-triggered method with integrated T1 estimation and the conventional triggered technique with dual-bolus. (**a**) Correlation between the two techniques show a very high correlation (r^2 = 0.964). (**b**) A Bland-Altman plot comparing the two methods, showing that there is a slight underestimation of MBF using the proposed method compared to conventional techniques. There are otherwise no discernible trends between the two techniques.